# Simulation, Optimization & Control of Styrene Bulk Polymerization in a Tubular Reactor

***Ghafoor Mohseni, Padideh; Shahrokhi, Mohammad\*+***
*Chemical and Petroleum Engineering Department, Sharif University of Technology,*
*P.O. Box: 11365-9465 Tehran, I.R. IRAN*

***Abedini, Hossein***
*Iran Polymer and Petrochemical Institute, P.O. Box: 14965-115 Tehran, I.R. IRAN*

**ABSTRACT:** *In this paper, optimization and control of a tubular reactor for thermal bulk post-polymerization of styrene have been investigated. By using the reactor mathematical model, static and dynamic simulations are carried out. Based on an objective function including polymer conversion and polydispersity, reactor optimal temperature profile has been obtained. In the absence of model mismatch, desired product characteristic can also be obtained by applying the corresponding reactor wall or jacket temperature profile. To achieve this temperature trajectory, reactor jacket is divided into three zones and jacket inlet temperatures are used as manipulated variables. Effectiveness of the proposed approach has been demonstrated through computer simulation. Furthermore for a special case of model mismatch, a method has been proposed which results in a near optimal profile.*

**KEY WORDS:** *Dynamic simulation, Tubular reactor, Styrene bulk polymerization, Optimization, Control.*

## INTRODUCTION

Polystyrene is one of the major commodity thermoplastics in the world. Continuous bulk styrene polymerization reactors are generally classified into two groups: the back mixed reactor and the Linear-Flow Reactor (LFR). Bulk styrene polymerization is always accompanied with a large heat generation and high viscosity. The choice of polymerization reactor depends on the desired polymer quality/quantity. Multiple reactor stages can be tailored in a number of ways to meet specific product needs. Most polystyrene licensors and/or producers still stay with two or more reactors in series to maintain production flexibility [1-4]. Due to the advantages of tubular reactors, regarding simple design and low cost, it is desired to use this type of reactor in polymerization processes [2, 4-6]. Studies of various aspects of polymerization in tubular reactors have been reported in the literature. Using different models for the process, the parametric sensitivity, stability, optimization and control have been considered [7-12]. Many theoretical and experimental works have been done

to study the feasibility and operability of bulk polymerization in tubular reactors [7-9]. In all of these works, the tubular rector has been considered as a post polymerization reactor and both axial and radial variations have been taken into account and a two-dimensional steady state model for the reactor has been considered. A commercial process for polystyrene production has been proposed by *Chen* [8]. It is desired to obtain maximum monomer conversion and a polymer with minimum possible polydispersity. *Costa et al.* [10] used the two dimensional steady state model proposed by *Chen* [8] and based on an objective function, optimal reactor wall temperatures through a multi objective optimization method has been obtained.

In industry, usually a series of reactors of different or similar types are used in polymerization processes [13]. The configuration proposed by *Chen* [8] for producing polystyrene consists of a CSTR (for polymerization up to 75%) followed by a tubular reactor to achieve product with about 90% conversion and more. Based on cumulative moment method, dynamic simulation of a two-stage continuous bulk styrene polymerization process is investigated by *Gharahni et al.* [14]. Also temperature control of auto-refrigerated continuous stirred tank reactor and tubular reactor by PI controllers are carried out, simultaneously.

In this work, radical thermal bulk polymerization of styrene in a tubular reactor, served as post polymerization, has been studied. In this paper, based on the work of *Chen* [8], first the mathematical model for the reactor is presented. In most of previous works static simulation and optimization have been considered but no practical way for implementation of optimal temperature profile along the reactor length had been mentioned. In this contribution, three optimization policies have been defined to minimize the selected objective function. Results of these three optimization problems provide reactor, wall and jacket temperature profile for the reactor. By using the static model, feasibility of implementation of optimization results have been studied. A control strategy is proposed to keep the desired temperature profile along the reactor length and its effectiveness has been shown trough simulation. Finally a special case of model mismatch has been taken into account and a strategy is proposed for handling the model uncertainty.

## MODELING

Based on mass and energy balances, the reactor mathematical model has been derived. It is assumed that static mixers are installed inside the reactor and therefore radial gradients of concentration, temperature and velocity are neglected. The flow pattern in the reactor is assumed to be plug flow [8]. Due to mixers effects, reactor model has less mathematical complexity and uniform residence times are obtained for the material inside the reactor (plug flow) and hence heterogeneity in the product is decreased. Furthermore, using of static mixers is an aid for effective heat removal from the reactor, which is crucial for highly exothermic reactions such as polymerization reactions.

By writing mass and energy balances, the following equations are obtained [8]:

$$\rho \frac{\partial \omega_m}{\partial t} = -\rho V_z \frac{\partial \omega_m}{\partial z} - R_p \tag{1}$$

$$c_p \rho \frac{\partial T}{\partial t} = -c_p \rho V_z \frac{\partial T}{\partial z} - R_p \Delta H + \frac{Q}{\pi R^2} \tag{2}$$

$$Q = h_i (2\pi R L_j)(T_w - T) = U_o (2\pi R_o L_j)(T_j - T) \tag{3}$$

$$V_j c_{p,j} \rho_j \frac{dT_j}{dt} = F_j c_{p,j}(T_{j,in} - T_j) - Q \tag{4}$$

The free-radical polymerization of styrene has already been extensively investigated in the literature. Therefore, rate constants and other kinetic parameters used in this work are those which are provided by other researchers [8, 15]. The kinetic mechanism considered here involves the following basic steps [15].
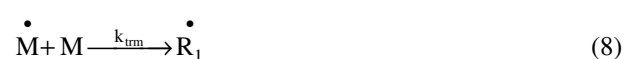
Thermal initiation:
$$3M \xrightarrow{k_i} 2R_1^\bullet \tag{5}$$

Propagation:
$$R_r^\bullet + M \xrightarrow{k_p} R_{r+1}^\bullet \tag{6}$$

Chain transfer to monomer:
$$d R_r^\bullet + M \xrightarrow{k_{trm}} P_r + M^\bullet \tag{7}$$

$$M^\bullet + M \xrightarrow{k_{trm}} R_1^\bullet \tag{8}$$

Termination by combination:
$$R_r^\bullet + R_s^\bullet \xrightarrow{k_{tc}} P_{r+s} \tag{9}$$

**Table 1: Physical and kinematics parameters [8, 10,15].**

| Kinetic model |
|---|

$$R_p = k_p(\rho w_m)\sqrt{\frac{2k_i(\rho w_m)^3}{k_{tc}}}$$

$$k_i = 2.019 \times 10^1 \exp\left(\frac{-13810}{T}\right) \ (m^6/kg^2)s$$

$$k_p = 1.009 \times 10^5 \exp\left(\frac{-3557}{T}\right) \ (m^3/s.kg)$$

$$k_{tc} = 2.205 \times 10^7 \exp\left(\frac{-844}{T}\right)\exp[-2\sum_{i=1}^{3} A_i(w_p)^i]\left(m^3/s.kg\right)$$

$$k_{trm} = 2.218 \times 10^4 \exp\left(\frac{-6377}{T}\right) \ \left(m^3/s.kg\right)$$

$$A_1 = 2.57 - 5.05 \times 10^{-3} T; A_2 = 9.56 - 1.76 \times 10^{-2} T; A_3 = -3.032 + 7.85 \times 10^{-3} T \quad [T] = K$$

| Formulas for molecular weight calculations |
|---|

$$\dot{\lambda}_0 = R_p(C_m + \frac{\beta}{2}) \quad , \quad \dot{\lambda}_1 = R_p(C_m + \beta + 1)$$

$$\dot{\lambda}_2 = R_p(2C_m + 3\beta)/(C_m + \beta)^2$$

$$\beta = \frac{k_{tc}R_p}{(k_p\rho w_m)^2}; C_m = \frac{k_{trm}}{k_p} + B_1 w_p$$

$$M_{n,inst} \approx 104\frac{\dot{\lambda}_1}{\dot{\lambda}_0}$$

$$M_{w,inst} \approx 104\frac{\dot{\lambda}_2}{\dot{\lambda}_1}$$

$$B_1 = \begin{cases} -1.013 \times 10^{-3} \log\left[\frac{473.12 - T}{202.5}\right] & T < 473K \\ \frac{0.01E_1}{(1 + 2E_1)} & T \geq 473K \end{cases}$$

$$E_1 = 0.9755 \exp\left[-12180\left(\frac{1}{T} - \frac{1}{473}\right)\right]$$

| Physical properties |
|---|

$$c_p = 1.884 \times 10^3 \ (J/kg.K) \ , \ \Delta H = -6.7 \times 10^5 \ (J/kg) \quad , \quad k = k_s w_m + k_{ps} w_p \ (W/m.K)$$

$$k_s = 4.187 \times 10^{-2}[2.72 - 2.8 \times 10^{-3}(T - 423) + 1.6 \times 10^{-5}(T - 423)^2] \ (W/m.K)$$

$$k_{ps} = 4.187 \times 10^{-2}[2.93 + 5.17 \times 10^{-3}(T - 353)] \ (W/m.K)$$

$$\rho = 845 - (T - 353) + [200 + (T - 353)]w_p \ (kg/m^3)$$

| Reactor dimensions & the feed properties |
|---|

| $d_i = 0.254\,m$ $L = 3 * 24.38\,m$ | $Q_m = 5682 \ kg\,h^{-1}$ | $PD_{feed} = 1.9878$ | $T_{feed} = 150$ | $\omega m_{feed} = 0.2918$ |

The required physical and system parameters properties are given in Table 1. Schematic diagram of the reactor is shown in Fig. 1.

## *Optimization*

By fixing feed characteristics (such as feed temperature, composition and mass flow rate), wall temperature and reactor length, the model can be solved and conversion as well as temperature profile along the reactor length are obtained. In an existing system, reactor dimensions are fixed. Usually the feed condition is fixed by the performance of the upstream reactor(s), especially in this case where the tubular reactor serves as a post polymerization unit. The remaining variables affecting the reactor performance are jacket temperatures which can be used as manipulated variables. To achieve maximum monomer conversion and minimum polydispersity, a performance index can be defined and based on

*Table 2: Results of reactor temperature optimization for $PD_{ref}$ = 2.4 and w = 0.5.*

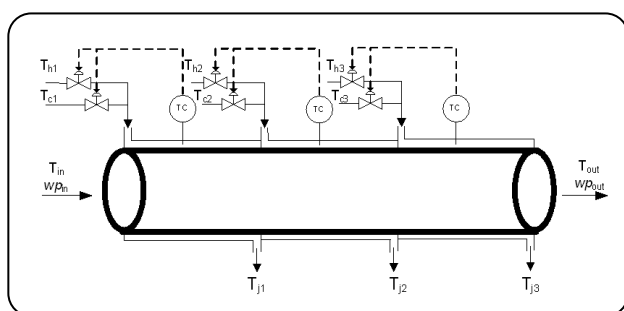| No. of sections | PD | $\omega m_f$ | PI |
|---|---|---|---|
| 3 | 2.4019 | 0.0717 | 0.0026 |
| 4 | 2.4020 | 0.0696 | 0.0024 |
| 5 | 2.4021 | 0.0685 | 0.0023 |
| 6 | 2.4021 | 0.0677 | 0.0023 |
| 7 | 2.4021 | 0.0672 | 0.0023 |
| 8 | 2.4021 | 0.0669 | 0.0022 |



*Fig.1: Schematic diagram of the reactor.*

this index the optimum reactor temperature profile will be obtained.

In [8], reactor wall temperature is chosen as the manipulated variable for temperature control. In [10], for achieving maximum monomer conversion and minimum polydispersity a performance index is defined and using a two-dimensional model, reactor wall temperature has been optimized. In this section, a brief discussion on obtaining the optimal reactor temperature profile is given.

As mentioned above, it is desired to obtain maximum monomer conversion with minimum polydispersity and, therefore the following objective function is considered:

$$PI = w(\omega m_f - \omega m_{ref})^2 + (1 - w)(PD_f - PD_{ref})^2 \qquad (10)$$

where $\omega m$ is monomer weight fraction, PD is polymer polydispersity and *w* is a weight factor. Subscripts f and ref stands for final and reference, respectively. For minimizing the above performance index (eq.10), the following three decision variables can be selected.

　a) reactor temperature
　b) reactor wall temperature
　c) reactor jacket temperature

Therefore, three optimization problems are formulated and discussed below. To solve the first optimization

problem, reactor length has been divided into m sections. Temperatures of these sections are determined such that the performance index (10) is minimized. The Genetic Algorithm Toolbox of MATLAB software with its default parameters are used for performing the optimization task. In solving the above optimization problems, there are some constraints that should be satisfied. For example if reactor temperature is considered as decision variable the following constraints should be taken into account.

　100°C <T< 220°C

For other cases, the following constraints on reactor wall and jacket temperatures are considered.

　100°C <$T_w$< 220°C
　100°C <$T_j$< 200°C

It should be noted that in performing optimization on reactor jacket, number of sections, m, is set to three, because according industrial process proposed by *Chen* [8] the reactor jacket has three heat transfer zones.

***Optimization results***

In solving optimization problems, as the number of reactor sections increases, it is expected that the discrete profile estimates the continuous profile more closely at the expense of significant raise of computation time. Table 2 and Fig. 2 show effect of number of sections in optimizing of the reactor temperature. As can be seen from Table 2, as number of sections exceeds five, no considerable changes are observed in polymer final characteristics. Therefore, to avoid increase of computation load, five zones have been chosen for further analysis. Effects of weight factor *w* on the optimization results for $PD_{ref}$ = $PD_{feed}$ and $PD_{ref}$ = 2.4 are shown in Tables 3 and 4 and Figs. 3 and 4.

It is seen from Table 3 that the value of the desired product polydispersity ($PD_{ref}$) has considerable effect

***Table 3: Results of reactor temprature optimization using five sections for $PD_{ref} = PD_{feed} = 1.9878$.***

| w | PD | $\omega m_f$ | PI |
|---|---|---|---|
| 0.1 | 2.0149 | 0.14257 | 0.0022 |
| 0.5 | 2.0548 | 0.11725 | 0.0083 |
| 0.7 | 2.0834 | 0.10601 | 0.0099 |
| 0.8 | 2.1066 | 0.09908 | 0.0101 |
| 0.9 | 2.1495 | 0.089528 | 0.0094 |
| 0.95 | 2.198 | 0.082083 | 0.0083 |

***Table 4: Results of reactor temprature optimization using five sections for PDref = 2.4.***

| w | PD | $\omega m_f$ | PI |
|---|---|---|---|
| 0.1 | 2.4004 | 0.0688 | 0.0005 |
| 0.5 | 2.4021 | 0.0685 | 0.0023 |
| 0.7 | 2.4048 | 0.0684 | 0.0033 |
| 0.8 | 2.408 | 0.0683 | 0.0037 |
| 0.9 | 2.4169 | 0.0681 | 0.0042 |
| 0.95 | 2.432 | 0.0677 | 0.0044 |
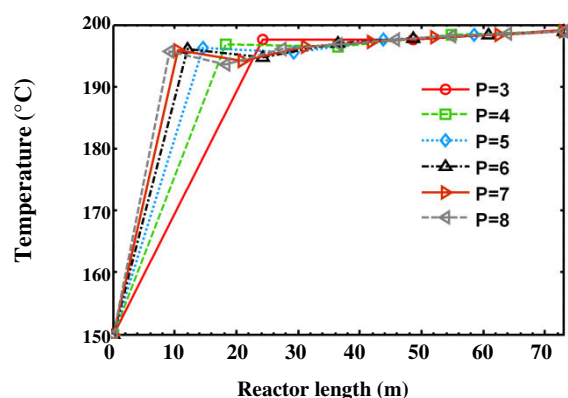


**Fig. 2: Reactor optimal temperature profile using different number of sections for $PD_{ref} = 2.4$ and w=0.5.**

on the optimization result. If $PD_{ref}$ is chosen to be the same as feed polydispersity, different weight factors lead into different results. As the value for $PD_{ref}$ is increased, effect of weight factor on the final conversion decreases considerably (Table 4).

The similar results for optimization wall temperature are given in Tables 5 and 6 and Figs. 5 and 6.

Results of optimization for reactor jacket temperature for w=0.5 and two different polydispersities are shown in Table and Fig. 7. By comparing results given in Tables 3, 5 and 7, it is concluded that the obtained polydispersity and monomer conversion from the optimal reactor temperature profile are almost the same as those obtained from optimum wall or jacket temperatures Therefore, by applying the optimum jacket temperature, the same results obtained from optimal reactor temperature profile can be achieved.

### Dynamic simulation and temperature control

For implementation of the desired optimal temperature profile along the reactor, the following control strategy is applied. The optimum jacket temperature of each section is used as its controller set point of the corresponding zone and the jacket inlet temperatures are considered as manipulated variables. Conventional PID controllers are used for control purposes [16]. For each section of the jacket, hot and cold service fluids are mixed to make the appropriate jacket inlet temperature. In other word, the real manipulated variables are the mass flow rates of hot and cold service streams. Dowtherm A is used as the service fluid inside the jackets.

It is assumed that the inlet feed condition to the reactor is known. This information is sent to a

*Table 5: Results of reactor wall temprature optimization for $PD_{ref} = PD_{feed} = 1.9878$.*

| w | PD | ωm$_f$ | PI | T$_{\omega_1}$ | T$_{\omega_2}$ | T$_{\omega_3}$ |
|------|--------|----------|----------|--------|--------|--------|
| 0.1 | 2.0063 | 0.15233 | 0.002646 | 149.43 | 125.82 | 149.11 |
| 0.5 | 2.0476 | 0.12265 | 0.009341 | 164.1 | 127.36 | 162.78 |
| 0.7 | 2.0767 | 0.11064 | 0.01097 | 170 | 128.73 | 168.7 |
| 0.8 | 2.1003 | 0.1034 | 0.011106 | 173.69 | 129.87 | 172.21 |
| 0.9 | 2.1436 | 0.093624 | 0.010332 | 178.99 | 131.93 | 176.59 |
| 0.95 | 2.1919 | 0.086233 | 0.009158 | 183.42 | 133.96 | 179.33 |

*Table 6: Results of reactor wall temprature optimization problem for $PD_{feed} = 2.4$.*

| w | PD | ωm$_f$ | PI | T$_{\omega_1}$ | T$_{\omega_2}$ | T$_{\omega_3}$ |
|------|--------|---------|----------|--------|--------|--------|
| 0.1 | 2.4003 | 0.07356 | 0.000541 | 192.14 | 139.07 | 182.23 |
| 0.5 | 2.4017 | 0.07353 | 0.000541 | 192.16 | 139.09 | 182.23 |
| 0.7 | 2.4037 | 0.07348 | 0.003784 | 192.18 | 139.13 | 182.24 |
| 0.8 | 2.4058 | 0.07344 | 0.004321 | 192.21 | 139.16 | 182.24 |
| 0.9 | 2.4127 | 0.0733 | 0.004852 | 192.29 | 139.27 | 182.25 |
| 0.95 | 2.4235 | 0.0731 | 0.005105 | 192.4 | 139.44 | 182.26 |
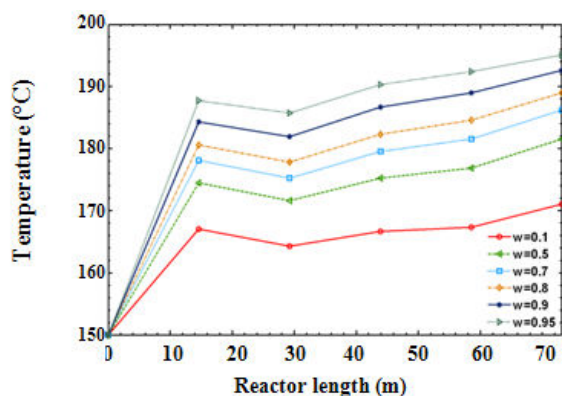


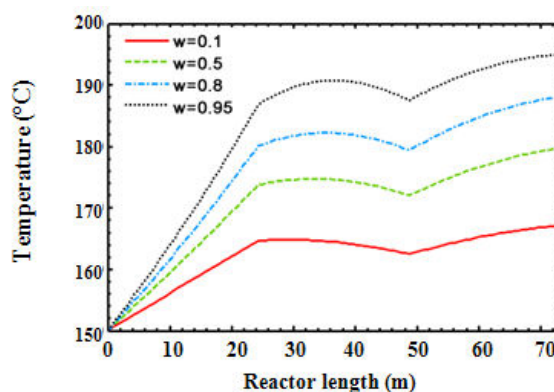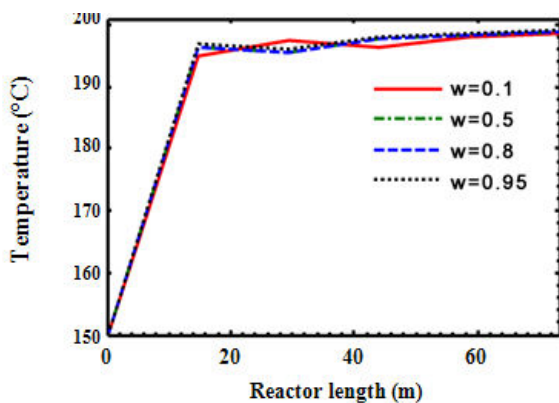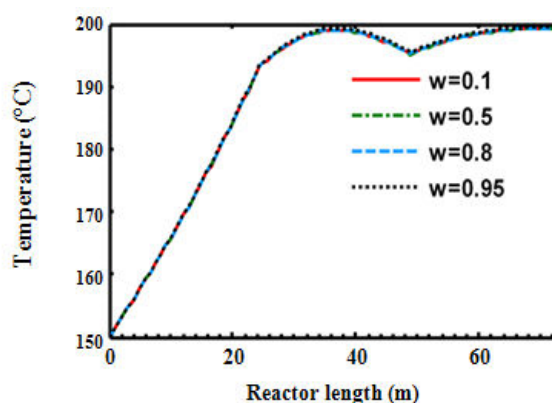*Fig. 3: Reactor optimal temperature profile for different values of w and $PD_{ref} = PD_{feed} = 1.9878$.*



*Fig. 5: Reactor temperature profile using optimum wall temperatures for $PD_{ref} = PD_{feed} = 1.9878$.*



*Fig. 4: Reactor optimal temperature profile for different values of w and $PD_{ref} = 2.4$.*



*Fig. 6: Reactor temperature profile using optimum wall temperatures $PD_{feed} = 2.4$.*

*Table 7: Results of reactor jacket temprature optimization for w=0.5.*

| PD$_{ref}$ | PD | ωm$_f$ | PI | T$_{j_1}$ | T$_{j_2}$ | T$_{j_3}$ |
|---|---|---|---|---|---|---|
| 2.2 | 2.2092 | 0.084428 | 0.0036063 | 191 | 113.27 | 174.12 |
| 1.9873 | 2.0476 | 0.12279 | 0.009357 | 165.2 | 110.07 | 157.45 |
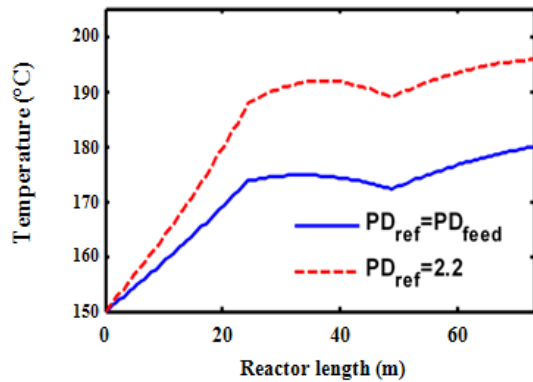


*Fig. 7: Reactor temperature profile using optimum reactor jacket temprature for w=0.5.*

computational unit that calculates set points for the different jacket zones by the a forementioned optimization method. In case of a change in the feed condition or product properties, the optimizer calculates the new optimal jacket temperatures for different jacket zones which are used as set points for the jacket controllers. To simulate the reactor dynamic behavior under control mode, Eqs. 1, 2, 4 and controller equations should be solved simultaneously.

Since the dynamic model is described by partial differential equations, using the orthogonal collocation method [16], the normalized version of equations 1, 2 are descretized in the axial direction as described below. The dimensionless variable x is defined as:

$$x = \frac{z}{L} \qquad (11)$$

The normalized version of Eqs. (1) , (2) are given below:

$$\frac{\partial \omega_m}{\partial t} = -\frac{V_z}{L}\frac{\partial \omega_m}{\partial x} - \frac{R_p}{\rho} \qquad (12)$$

$$\frac{\partial T}{\partial t} = -\frac{V_z}{L}\frac{\partial T}{\partial x} - \frac{R_p \Delta H}{c_p \rho} + \frac{\overline{U}_0 (2R_0)(\overline{T}_{j,k} - T)}{R_i^2 \rho c_p} \qquad (13)$$

k=1,2,...,n

The discritized version of Eqs. (12), (13) are as follows:

$$\frac{d\omega_m(i)}{dt} = -\frac{V_z(i)}{L}\sum_{j=1}^{N+1} A(i,j)\omega_m(j) - \frac{R_p(i)}{\rho(i)} \qquad (14)$$

i=2,3,...,N+1

$$\frac{dT(i)}{dt} = -\frac{V_z(i)}{L}\sum_{j=1}^{N+1} A(i,j)T(j) - \frac{R_p(i)\Delta H}{c_p\rho(i)} + \qquad (15)$$

$$\frac{\overline{U}_0(2R_0)(\overline{T}_{j,k} - T(i))}{R_i^2\rho(i)c_p} \qquad k=1,2,...,n \qquad i=2,3,...,N+1$$

The corresponding boundary conditions for different zone are:

$$\begin{cases} \omega_{m_1}\big|_{x_1=1} = \omega_{m_2}\big|_{x_2=0} \\ \omega_{m_2}\big|_{x_2=1} = \omega_{m_3}\big|_{x_3=0} \end{cases} \Rightarrow \begin{cases} \omega_{m_1}(N+1) = \omega_{m_2}(1) \\ \omega_{m_2}(N+1) = \omega_{m_3}(1) \end{cases} \qquad (16)$$

$$\begin{cases} T_1\big|_{x_1=1} = T_2\big|_{x_2=0} \\ T_2\big|_{x_2=1} = T_3\big|_{x_3=0} \end{cases} \Rightarrow \begin{cases} T_1(N+1) = T_2(1) \\ T_2(N+1) = T_3(1) \end{cases} \qquad (17)$$

The resulting ordinary differential Eqs. (4), (14), (15) and controller equation are solved simultaneously.

### Model mismatch

In presence of model mismatch, the desired temperature profile can not be established in the reactor because the calculated profile has been obtained from the reactor wrong model. Error in calculating the heat transfer coefficient is a common type of modeling error. To reduce effect of this error, the following correction technique is proposed [16].

1- The temperature at the outlet of reactor is measured. The difference between desired and actual temperatures at the end of reactor is calculated ( $e_L = T_{d,out} - T_{out}$ ).

2- Reactor length is divided into m sections. It is assumed that the reactor inlet temperature is measured.

Errors at the end of each section are estimated using the following equation.

$$e_i = \frac{e_L}{L} z_i \quad i = 1, 2, ..., m-1 \qquad (18)$$

3- If it is the first trial, by adding the calculated errors to the desired temperatures at the end of each section, the estimated desired temperatures at each section are obtained. A proper curve-fitting method will provide the estimated temperature profile. The mirror image of this estimated profile is the virtual desired temperature profile. In trials other than the first one, the virtual profile is obtained by the same procedure and using the previous virtual profile.

4- Using the virtual optimal temperature trajectory and the reactor model, the corresponding virtual jacket optimal temperature profile is obtained. By discredization this profile into three zones, the new set points for different jacket zones are obtained. After applying these set points by controllers and reaching steady state, the reactor outlet temperature is measured.

5- Steps 1 through 4 are repeated until $e_L$ becomes less than a predetermined value.

### Dynamic simulation results

To evaluate the control system performance, feed temperature is decreased to 140°C at t=4500 seconds, and returned to its initial value (150°C) at t=14500 seconds. The results are shown in Fig. 8. As can be seen, after each feed temperature change, the steady reactor temperature profiles are very close to the optimal profile, which demonstrates the effectiveness of the applied control scheme.

For checking the performance of the proposed control scheme for set point tracking, polydispersity is changed from 2.05 to 2.2 at t=5000 seconds. The results are shown in Fig. 9. As can be seen, the final temperature profile is very close to the optimal profile and the desired polydispersity is almost achieved.

To show the effectiveness of the proposed scheme in case of model mismatch, the simulation results for decreasing the overall heat transfer coefficient by 40%, are shown in Fig. 10. As can be seen the reactor outlet temperature has approached to the optimal outlet temperature and final monomer weight fraction and polydispersity are almost the same as desired ones.
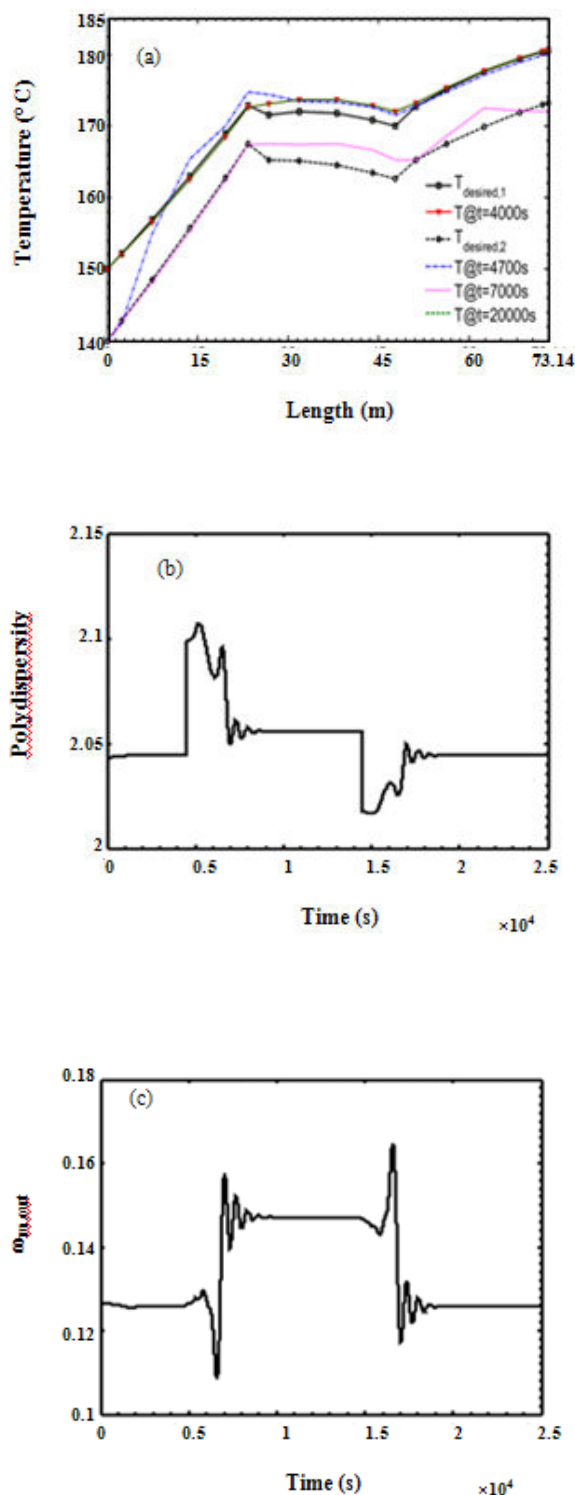


*Fig. 8: Closed-loop responses for step changes in feed temperature a) Desired profiles and transient reactor temperature b) Polydispersity versus time c) Outlet monomer fraction versus time.*
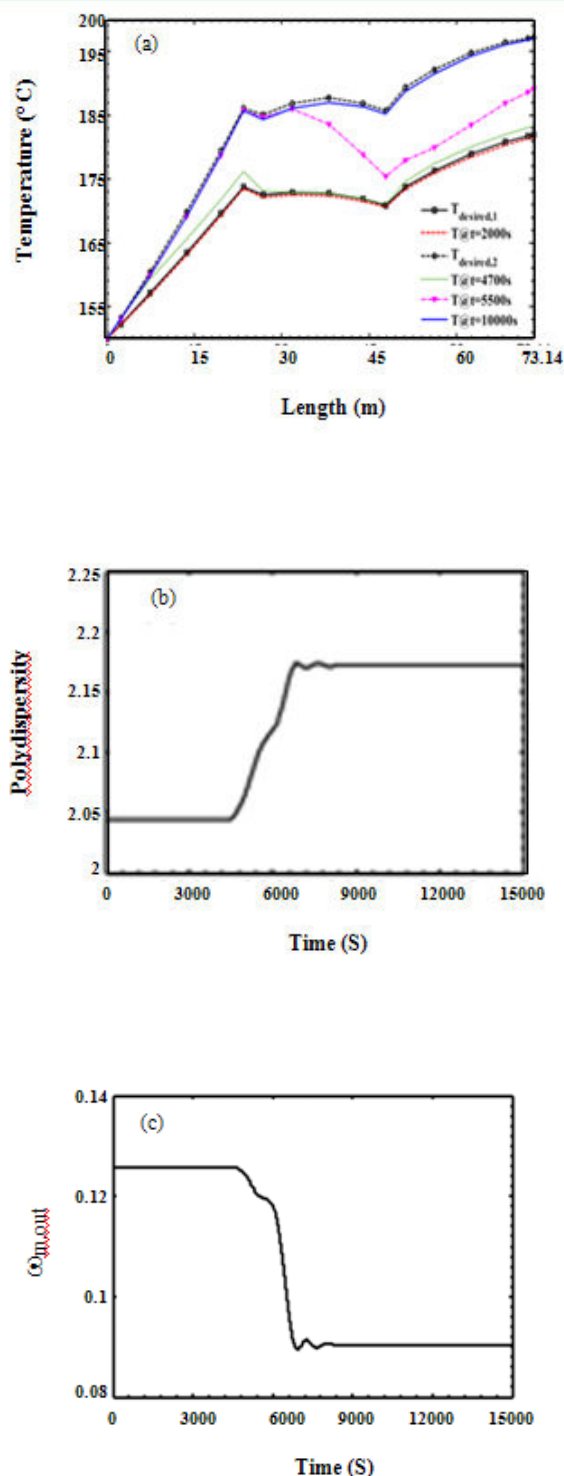
*Fig. 9: Closed-loop responses for a change in product polydispersity, Desired profiles and transient reactor temperature b) Polydispersity versus time c) Outlet monomer fraction versus time.*

Note: If in addition to monomer conversion and polydispersity ,polymer molecular weight is also to be fixed, one can modify the objective function(5) into the following form:

$$PI = w_1(\omega m_f - \omega m_{ref})^2 + w_2(PD_f - PD_{ref})^2 + \qquad (19)$$

$$w_3(1 - \frac{Mn_f}{Mn_{ref}})^2$$

As can be seen, the desired number average molecular weight, $Mn_f$, is included in objective function. $w_i$s are weights that can be fixed according to the importance of polymer properties(monomer conversion , polydispersity and molecular weight). For example if one select $w_1 = w_2 = w_3 = \frac{1}{3}$, and set $Mn_{ref} = 92000$, $\omega m_{ref} = 0$, $PD_{ref} = 2.45$, the optimal wall temperatures will be $T_{w1}$ =172.6, $T_{w2}$=155.9, $T_{w3}$=181.5. The above temperatures are used as controller set points.

**CONCLUSIONS**

In this work, simulation, optimization and control of styrene free radical, bulk thermal polymerization in a tubular reactor has been studied. Usually this reactor serves as a postpolymerizer unit. It is assumed that static mixers are installed inside the reactor to provide plug flow. Using the first principles and the reaction kinetics, mathematical model for the reactor is obtained. In order to have a desired product regarding monomer conversion and polymer polydispersity at the reactor outlet, a specific temperature profile must be kept along the reactor length. Based on an objective function, which includes final monomer weight fraction and polymer polydispersity, optimal reactor temperature profile has been obtained. Since measuring temperature inside the reactor is a difficult task, corresponding jacket temperature profile has been calculated and used for control purposes. Simulation results indicate that controlling the different jacket zones temperatures at their desired values, results in almost optimal reactor temperature profile. In case of a special type of model mismatch, a scheme has been suggested to reduce the effect of model uncertainty. Effectiveness of the proposed control strategy has been demonstrated through computer simulation.
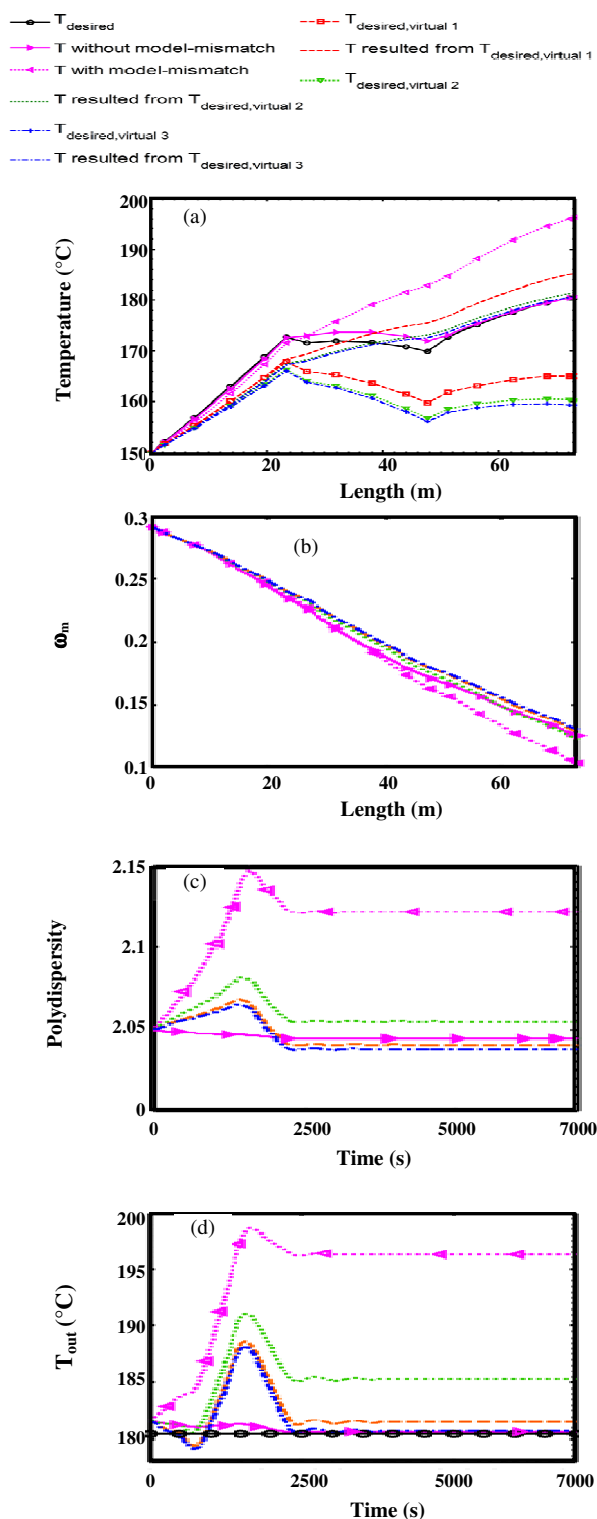
**Fig. 10: Closed-loop responses for -40% error in heat transfer coefficient; a) Reactor temperature profile variations, b) monomer fraction profiles corresponding to each temperature profile in plot a, c) Polydispersity variations, d) Reactor outlet temperature versus time.**

## Notations

| | |
|---|---|
| $C_p$ | Specific heat of monomer, polymer or mixture, J/kgK |
| $C_{p,j}$ | Specific heat of the service fluid |
| $\Delta H$ | Heat of reaction, J/kg |
| $F_j$ | Mass flow rate to the jacket, kg/s |
| $h_i$ | Heat coefficient inside the reactor, W/m$^2$K |
| $k$ | Thermal conductivity of polystyrene, styrene or mixture, W/mK |
| $k_i$ | Initiation rate constant, m$^6$/kg$^2$s |
| $k_p$ | Propagation rate constant, m$^3$/s.kg |
| $k_{tc}$ | Termination rate constant, m$^3$/s.kg |
| $L$ | Reactor length, m |
| $L_j$ | Jacket length, m |
| $M_n$ | Number average molecular weight, kg/kgmol |
| $M_w$ | Weight average molecular weight, kg/kgmol |
| $N$ | Number of Collocation Points |
| $R_i$ | Reactor radius, m |
| $R_o$ | Jacket radius, m |
| $R_p$ | Rate of polymerization |
| $T$ | Reactor's temperature, K |
| $T_j$ | Jacket temperature, K |
| $T_w$ | Reactor wall temperature, K |
| $T$ | Time, s |
| $U_o$ | External overall heat transfer coefficient, W/m$^2$K |
| $V_z$ | Axial velocity, m/s |
| $V$ | Reactor Volume, m$^3$ |
| $w_m$ | Styrene weight fraction |
| $w_p$ | Polystyrene weight fraction |
| $x$ | Normalized axial position |
| $z$ | Axial position, m |

## *Greek Symbols*

| | |
|---|---|
| $\Delta H$ | Heat of reaction, J/kg |
| $\mu$ | Viscosity, Pas |
| $\lambda_k$ | Rate of k_th moment of polymer distribution |
| $\rho$ | Density of styrene_polystyrene mixture, kg/m$^3$ |
| $\omega$ | Weighting factor in the objective function |

## REFERENCES

[1] Chen C.C., Continuous Production of Solid Polystyrene in Back-Mixed and Linear-Flow Reactors, *Polym. Eng. And Sci.*, **40**, p. 441 (2000).

[2] Makwana Y., Moudgalyk K. M., and Khakhar D.V., Modeling of Industrial Styrene Polymerization Reactors, *Polym. Eng. And Sci.*, **37**, p. 1073 (1997).

[3]   Bhat S.A., Sharma R., Santosh K., Gupta S.K., Simulation and Optimization of the Continuous Tower Process for Styrene Polymerization, *Journal of Applied Polymer Science*, **94**, p. 775 (2004).

[4]   Nauman E.B., "Chemical Reactor Design, Optimization and Scale Up", McGraw-Hill, (2001).

[5]   Zhang M., Ray W.H., "Odeling of Living Free-Radical Polymerization Processes. II. Tubular Reactors, *Journal of Applied Polymer Science*, **86**, p. 1047 (2002).

[6]   Beuermann S., Buback M., Gadermann M., Jurgens M., Saggu D.P., Tubular Reactor Synthesis of Styrene-Methacrylate Copolymers in Solution with Supercritical Carbon Dioxide, *J. of Supercritical Fluids*, **39** , p. 246 (2006).

[7]   Agarwal S.S., Kleinstreuer C., Analysis of Styrene Polymerization in a Continuous Flow Tubular Reactor, *Chemical Engineering Science*, **41**, p. 3101 (1986).

[8]   Chen C.C., A Continuous Bulk Polymerization Process for Crystal Polystyrene, *Polymer-Plastic Technology of Engineering*, **33**, p. 55 (1994).

[9]   Chen C.C., Nauman E.B., Verification of a Complex, Variable Viscosity Model for a Tubular Polymerization Reactor, *Chemical Engineering Science*, **44**, p. 179 (1989).

[10]  Costa E.F., Lage P.L.C., Biscaia E.C., On the Numerical Solution and Optimization of Styrene Polymerization in Tubular Reactors, *Computers & Chemical Engineering*, **27**, p. 1591 (2003).

[11]  Vega M.P., Lima E.L., Pinto J.C., Use of Bifurcation Analysis for Development of Nonlinear Models for Control Applications, *Chemical Engineering Science*, **63**, p. 5129 (2008).

[12]  Wallis J.P., Ritter R.A., Andre H., Continuous Production of Polystyrene in a Tubular Reactor: Part II, *AIChE Journal*, **21**, p. 691 (1975).

[13]  Process Economic Program, SRI International, 39D, "Polystyrene", (2001).

[14]  Gharaghani M., Abedini H., Parvazinia M., Dynamic Simulation and Control of Auto-Refrigerated CSTR and Tubular Reactor for Bulk Styrene Polymerization, *Chem. Eng. Res. Des.*, doi:10.1016/j.cherd.2012.01.019 (2012).

[15]  Hui A.W., Hamielec A.E., Thermal Polymerization of Styrene at High Conversions and Temperatures- An Experimental Study, *J. Appl. Polym. Sci.*, **16**, p. 749 (1972).

[16]  Shahrokhi M., Nejati A., Optimal Temperature Control of Thermal Cracking Reactor, *Ind. Eng. Chem. Res.*, **41**, p. 6572 (2002).

[17]  Rice R., Do D.D., "Applied Mathematics and Modeling for Chemical Engineers", New York Wiley, (1994).